$$v = 1.4 \left(\frac{Fgz}{\rho c_p T}\right)^{1/3} \quad (1)$$

$$\delta T = 1.3 \left(\frac{F}{\rho c_p}\right)^{2/3} \left(\frac{gz}{T}\right)^{-1/3} \quad (2)$$

For Earth with $F = 1000$ W m$^{-2}$ and $z = 2$ m, we obtain $v = 0.54$ m s$^{-1}$ and $\delta T = 3.1$ K. In contrast, Sinclair (*3*) measures $v = 10$ m s$^{-1}$ and $\delta T = 5$ K at $z = 2$ m for several large dust devils. We conjecture that the similarity relations fail because the mixed layer thickness $h$ is also entering the problem (*15*, pp. 137–138). Possibly the ground-to-air temperature difference $\Delta T$ is entering too. In any case, we adopt the formula

$$v_d = 0.5 \left(\frac{gh\Delta T}{T}\right)^{1/2} \quad (3)$$

as the velocity in a large dust devil. This expression is consistent with the similarity relations if we substitute $h$ for $z$ and $\Delta T$ for $\delta T$, eliminating $F/\rho c_p$ from the two equations, but the numerical constant is different. The constant above was chosen to give $v = 10$ m s$^{-1}$ when $g = 10$ m s$^{-2}$, $h = 600$ m, $\Delta T = 22$ K, and $T = 320$ K (*3*). The above equation says that kinetic energy is proportional to the potential energy involved in lifting a parcel with vertical acceleration $g\Delta T/T$ through a distance $h$. The $h^{1/2}$ dependence is also consistent with the empirical results of Ryan and Carroll (*1*), and the numerical constant is consistent with the strongest dust devils they encountered.

The mixed layer is the zone of buoyancy-generated turbulence that develops during the day above the unstable surface layer (*15*). On Earth, its thickness is limited by the heat capacity of the atmosphere and is of order $h = F/(\rho c_p \Delta T \Omega) \approx 600$ m, where $F$ is the solar flux reaching the ground. On Mars and Triton the above expression gives $h > 10$ km, indicating that the mixed layer could occupy most of the atmosphere. A more conservative estimate is that $h$ is equal to the heights of the plumes, 6 km for Mars (*6*) and 8 km for Triton (*7*). With these choices and with $\Delta T/T = 0.25$, we obtain $v_d = 40$ m s$^{-1}$ for Mars and 20 m s$^{-1}$ for Triton.

It is not clear that winds of order 20 m s$^{-1}$ could pick up material on Triton. The friction velocity $u_*$ is likely to be 10 to 20 times smaller than the wind above the boundary layer (*15*, p. 168). If the latter is 20 m s$^{-1}$, the friction velocity is only 1 or 2 m s$^{-1}$. Then the interparticle cohesion forces would have to be $10^3$ to $10^4$ times smaller on Triton than on Earth, according to the formula of Sagan and Chyba (*16*). They regard such differences as possible. Certainly, the difference in temperature would tend to make water ice particles much less cohesive on Triton than on Earth.

The alternative is that the plumes are indeed geysers or eruptions of some sort (*17*). If so, the eruptions are fundamentally different from those on Io. The plume does not spread into an umbrella shape, nor does it rise above the atmosphere like the hypervelocity jets of Io. Instead, it spreads out horizontally at 8-km altitude, as if the density structure of the atmosphere were controlling its rise. In short, the plumes look like buoyant columns (*7, 8*), and their narrowness makes them look like atmospheric vortices. They might be dust devils.


REFERENCES AND NOTES

1. J. A. Ryan and J. J. Carroll, *J. Geophys. Res.* **75**, 531 (1970).
2. R. L. Ives, *Bull. Am. Meteorol. Soc.* **28**, 168 (1947).
3. P. C. Sinclair, *J. Atmos. Sci.* **30**, 1599 (1973).
4. ———, *J. Appl. Meteorol.* **8**, 32 (1969); J. A. Ryan, *J. Geophys. Res.* **77**, 7133 (1972).
5. P. Dergarabedian and F. Fendell, *Tellus* **23**, 5 (1970).
6. P. Thomas and P. J. Gierasch, *Science* **230**, 175 (1985).
7. B. A. Smith *et al.*, *ibid.* **246**, 1422 (1989); L. A. Soderblom *et al.*, *ibid.* **250**, 410 (1990).
8. R. V. Yelle *et al.*, *Icarus*, in press.
9. B. Conrath *et al.*, *Science* **246**, 1454 (1989).
10. A. L. Broadfoot *et al.*, *ibid.*, p. 1459.
11. A. P. Ingersoll, *Nature* **344**, 315 (1990).
12. O. Hansen, *Icarus* **18**, 237 (1973).
13. A. McEwen *et al.*, *Geophys. Res. Lett.*, in press.
14. G. L. Tyler *et al.*, *Science* **246**, 1466 (1989).
15. S. P. Arya, *Introduction to Micrometeorology* (Academic Press, San Diego, 1988).
16. C. Sagan and C. Chyba, *Nature* **346**, 546 (1990).
17. R. H. Brown *et al.*, *Science* **250**, 431 (1990); R. L. Kirk *et al.*, *ibid.*, p. 424.


18. We thank P. Gierasch and R. Yelle for useful suggestions. This work was supported by the NASA planetary atmosphere program (NAGW-58) and by Voyager Project funds. This is contribution number 4905 of the Division of Geological and Planetary Sciences, California Institute of Technology.

9 August 1990; accepted 20 September 1990


# The Impact Cratering Record on Triton


ROBERT G. STROM, STEVEN K. CROFT, JOSEPH M. BOYCE



**Impact craters on Triton are scarce owing to the relatively recent resurfacing by icy melts. The most heavily cratered surface has a crater density about the same as the lunar maria. The transition diameter from simple to complex craters occurs at a diameter of about 11 kilometers, and the depth-diameter relationship is similar to that of other icy satellites when gravity is taken into account. The crater size-frequency distribution has a differential −3 slope (cumulative −2 slope) and is the same as that for the fresh crater population on Miranda. The most heavily cratered region is on the leading hemisphere in Triton's orbit. Triton may have a leading-trailing asymmetry in its crater population. Based primarily on the similarity of size distributions on Triton and Miranda and the relatively young surface on Triton, the source of Triton's craters is probably comets. The very peculiar size distribution of sharp craters on the "cantaloupe" terrain and other evidence suggests they are volcanic explosion craters.**


IMPACT CRATERS ON TRITON ARE RARE to nearly absent at the 3 to 1.8 km resolutions acquired on the mapping sequence of Voyager 2. The highest resolution (1.8 to 0.8 km) terminator images have various degrees of smear and, therefore, crater counts have not yet been performed. When these images have been desmeared they should provide useful information on the small crater population and extend the size distribution downward.

Although extensive resurfacing has left only a few late-forming impact craters, there are still enough craters to provide information on the size-frequency distribution and to locally derive relative terrain ages. However, the diameter range over which the size distribution can be reliably determined is very limited, making comparisons with most other outer planet satellites difficult to impossible. Furthermore, the identification of impact craters on certain terrains is extremely difficult due either to the complex nature of the terrain or the high sun angle under which it was viewed.

Triton's surface records the relatively recent impacts which have occurred since it was extensively resurfaced by internal processes. No reliable record of an early intense bombardment remains on the part of Triton imaged at relatively high resolution. The largest uncontested impact crater viewed by Voyager 2 on Triton (Mazomba) is only about 27 km in diameter. There are several larger quasi-circular features, but they may be of internal origin, particularly since there are numerous acknowledged circular volcanic structures present in most areas of the


R. G. Strom and S. K. Croft, Lunar and Planetary Laboratory, University of Arizona, Tucson, AZ 85721. J. M. Boyce, NASA Headquarters, Washington, DC 20546.

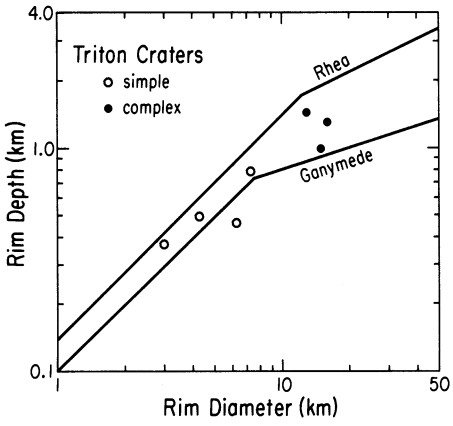


**Fig. 1.** Depth-diameter plot for craters on Triton. The symbols represent the craters on Triton while the solid lines are least-squares fits to craters on Ganymede and Rhea (*2*), icy satellites that bracket Triton in surface gravity (1.43 m $s^{-2}$ on Ganymede, 0.76 m $s^{-2}$ on Triton, and 0.28 m $s^{-2}$ on Rhea). The change in slope for the solid curves correspond approximately to the simple-complex morphology transitions on the respective satellites.

satellite. This report discusses the cratering record in more detail than the *Science* (*1*) article which presented the overall preliminary results of the imaging experiment.

Fresh impact craters on Triton have morphologies similar to those on other icy satellites seen at comparable resolutions. Morphologies include both simple (sharp-rims and bowl-shaped interiors) and complex craters (flat-floored with central peaks). The transition diameter from simple to complex craters occurs at a diameter of about 11 ± 2 km. This is consistent with the transition diameters for craters on other icy satellites when their surface gravities are taken into account (*2*). The depth/diameter relationships are also similar to those observed on other icy satellites, as may be seen in Fig. 1. The depth data are sparse (only 7 depths derived from shadow measurements) and the uncertainties large (estimated at 10 to 15% in both depth and diameter). However, the logarithmic slope for the simple craters is consistent with the value of unity found for simple craters on other bodies (*2*), and the depths of the complex craters are consistent with a slight change in slope near the diameter of the transition from simple to complex morphology, behavior similar to that found for the depths of complex craters on other icy bodies.

Triton's impact craters do not show recognizable ejecta blankets or interior terraces, but this is probably due to the low resolution of the images. Fresh lunar craters of comparable diameter also do not show ejecta blankets or terracing at similar resolutions. The fresh craters also do not display either light or dark rays, although the resolution is sufficient to discern them. This could be due to the high albedo of the surface or darkening of light rays by radiation or micrometeorite gardening. Several large circular features up to 50 km in diameter occur in the frost-covered southern hemisphere and near the "cantaloupe" terrain. Although these could be impact craters dating from an earlier period of heavy bombardment, they have been so degraded and modified by internal processes that all impact morphological signatures, except their circularity, have been erased. With the limited information available it is impossible to prove an impact origin.

The low crater density combined with the relatively low resolution of the images provides only marginally significant size-frequency data except in the most heavily cratered area of the leading hemisphere. Furthermore, the diameter range over which the curve can be determined is limited to about 3 to 20 km. Eventually, counts on the highest resolution smeared images could extend this range down to about 1 km.

The surface of Triton covered by the mapping sequence was divided into four areas indicated by the solid outlines in figure 33 of Smith *et al.* (*1*). Area 1 is the most heavily cratered region and straddles the equator between about 30° and 70° longitude. Area 2 is the most lightly cratered region. It is just west of area 1, between about 0° and 30° longitude, and includes the lake-like smooth plains. Area 3 is west of area 2 and largely comprises the "cantaloupe" terrain. Area 4 is the portion of the frost-covered southern hemisphere south of areas 1 and 2 down to about latitude 40° south.

The "cantaloupe" terrain (area 3) presents a special problem for impact crater recognition. Because of the rugged nature of the terrain and the low resolution (about 3 km) at which most of it was imaged, impact craters are extremely difficult to recognize with any degree of certainty. There are a number of sharp circular to irregular bowl-shaped craters scattered throughout the terrain, but many of these structures are in pairs or in widely dispersed strings. Counts of these structures yield a very peculiar size-frequency distribution with the vast majority of "craters" occurring over a very narrow diameter range (about 6 to 11 km). Figure 2 is an *R* plot (*3*) of this size distribution compared to that of area 1. Because the curve is very different from that of area 1 and is peaked at a narrow diameter range, we believe these structures are not primary impact craters. Furthermore, a comparison of features mapped as impact craters on the low-resolution images with the same features shown on the one unsmeared high-resolution image covering a portion of this

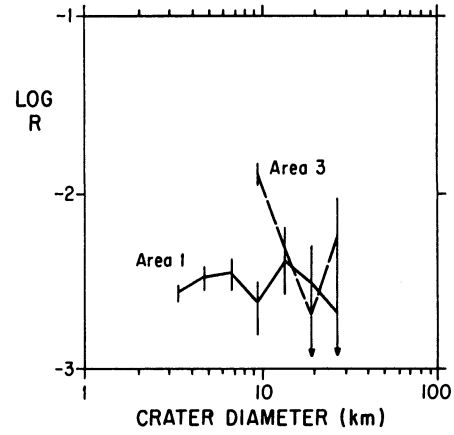


**Fig. 2.** *R* plot (*3*) of the size-frequency distribution for "craters" on the "cantaloupe" terrain (area 3) compared to area 1. Most craters occur over a very narrow diameter range suggesting they are mostly internal in origin. See text for explanation.

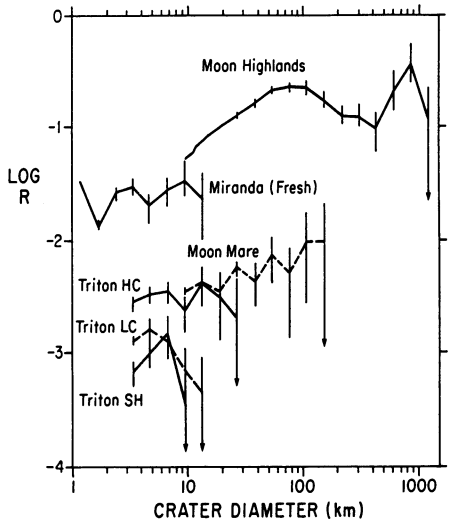


**Fig. 3.** *R* plot (*3*) of the crater size-frequency distribution for area 1 (Triton HC), area 2 (Triton LC), and area 4 (Triton SH) compared with the fresh crater population on Miranda, the lunar highlands, and the lunar post-mare.

terrain shows that they do not have morphologies typical of fresh impact craters. Although they could be secondary impacts from some large crater beyond the limb, it is more likely they are volcanic explosion craters (*4*). In addition, a distinct population of large (20 to 40 km in diameter) crater-like features termed "cavi" occur in the eastern portion of the cantaloupe terrain. These features are interpreted as endogenic in origin because of their nonrandom distribution, distinct size range, and morphologies. The range of morphologies, however, includes a few cavi similar enough to impact craters that an undisputed endogenic origin cannot be maintained, further clouding the accuracy of crater counts in the cantaloupe terrain.

Figure 3 is an *R* plot of the crater size-frequency distribution for areas 1 (Triton

**Table 1.** Statistical data for fresh craters on Triton and Miranda. The craters on Triton were counted in area 1 (total surface area of 978,900 km$^2$), in the leading hemisphere. The craters on Miranda were counted in the heavily cratered terrain, which extends over most of the observed surface (total surface area, 64,000 km$^2$).

| Diameter range (km) | Mean diameter (km) | Triton number | Miranda number |
|---|---|---|---|
| 1 – 1.4 | 1.19 | — | 518 |
| 1.4– 2 | 1.68 | — | 102 |
| 2 – 2.8 | 2.38 | — | 108 |
| 2.8– 4 | 3.36 | 82 | 61 |
| 4 – 5.6 | 4.76 | 51 | 20 |
| 5.6– 8 | 6.73 | 27 | 14 |
| 8 –11.3 | 9.51 | 9 | 9 |
| 11.3–16 | 13.4 | 8 | 3 |
| 16 –22.6 | 19.0 | 3 | — |
| 22.6–32 | 26.9 | 1 | — |

HC), 2 (Triton LC), and 4 (Triton SH) compared with those of the lunar highlands, the lunar post-mare and the fresh crater population on Miranda. Table 1 lists the crater counts for Triton's heavily cratered region (area 1) and for the fresh crater population on Miranda (*5*). The crater density for the most heavily cratered terrain (area 1; HC) is essentially the same as that of the lunar post-mare craters over the same diameter range. Although the statistics are poor, both area 2 (LC) and area 4 (SH) are at about the same longitude and have the same crater density, suggesting that the frost-covered southern hemisphere and the region containing the lake-like smooth plains are about the same age. They have a crater density about half that of area 1. Furthermore, the crater density on the lake-like smooth plains near the terminator is much lower (only two craters) than on the smooth terrain in the highlands immediately to the east, indicating the lake-like smooth plains are younger.

Although area 1 is the most heavily cratered region on Triton's imaged surface, it is not necessarily the oldest surface. This part of Triton lies in the leading hemisphere in its orbit around Neptune and, therefore, impacts will be more frequent and at higher velocities than elsewhere on the satellite. The crater frequency should decrease from the apex to the antapex of motion as observed (note that due to the limited coverage of high-resolution imagery of Triton, distance from the apex is roughly equivalent to longitude). Furthermore, the three largest observed craters all occur within about 50 km of each other and nearer the apex of motion than most other craters in the region. Therefore, the relatively high crater density in area 1 compared to other areas could be wholly or partly due to a leading-trailing asymmetry in the crater production rate. If this is the case then determining relative ages from crater abundances on relatively widely separated terrains could lead to erroneous results. This method of age dating should only be attempted for adjacent terrains at similar longitudes.

We attempted a more refined estimate of the leading-trailing asymmetry by counting craters in the areas denoted by dashed lines in figure 33 of Smith *et al.* (*1*). These areas were chosen to encompass similar geologic provinces to eliminate real geologic age differences as much as possible. The approximate bounding longitudes and cumulative number of craters above 4 km in diameter of each area are, respectively: area 6 (60° to 57°) and 13 ± 4 per $10^6$ km$^2$, area 7 (30° to 60°) and 12 ± 3 per $10^6$ km$^2$, and area 8 (0° to 30°) and 6 ± 2 per $10^6$ km$^2$. Admittedly the statistics are marginal and do not conclusively indicate a leading-trailing asymmetry. However, the factor of 2 lower crater density between area 8 and areas 6 and 7 is broadly consistent with a decrease in crater density between the apex of motion and the boundary between the leading and trailing hemispheres.

A comparison of Triton's and Miranda's cratering record sheds some light on the origin of the impacting objects. The crater statistics in lightly cratered areas are too poor and have too small a diameter range to be much help in determining the crater size-frequency distribution, thus only Triton's most heavily cratered terrain (area 1) is considered a fairly reliable indication of the crater size-frequency distribution. Figure 3 shows the impact crater size-frequency distribution for the craters in area 1 (HC) on Triton and for fresh craters on Miranda (*5*). Both distributions have a differential −3 slope, and an upper diameter cutoff of about 20 km. The density of the fresh craters on Miranda is about an order of magnitude higher than the craters on Triton. The distribution for craters on the lunar maria, also shown in Fig. 3, has a slope and density similar to Triton's, but the upper diameter cutoff is near 100 km. The largest undisputed crater on Triton is 27 km in diameter, and Triton is large enough that craters larger than 30 km should occur if sufficiently large projectiles were present in the impactor population. Thus the lower cutoff for crater (and impactor) sizes on Triton and Miranda relative to the moon is apparently real and reflects a real difference in the respective impactor size distributions. On the moon this population must contain a substantial number of asteroids which are not present at Uranus and Neptune.

In addition to similar population statistics, both the craters on Triton and the fresh craters on Miranda (*6*) may have leading-trailing asymmetries. Since Miranda is in prograde orbit, the leading-trailing asymmetry most likely indicates a source population external to the Uranian system: that is, comets. The leading-trailing asymmetry for Triton's craters is also consistent with a cometary origin, but unfortunately not diagnostic. Since Triton's orbit is retrograde, planetocentric objects in prograde orbits (which were almost certainly present) will also preferentially impact on its leading hemisphere. This is not inconsistent with capture models for Triton (*7*), which propose an initial eccentric orbit and tidal heating followed by circularization of the orbit and sweepup of objects in prograde orbits. However, because of the similar population statistics and the relative youth of Triton's surface (post any tidal heating episode) we favor a cometary origin for the impacting objects. If this is true then comets have a differential −3 size distribution, at least for craters less than about 20 km. Crater populations elsewhere in the outer solar system that differ from a −3 slope over this diameter range probably have a different origin, planetocentric, for example. Unfortunately, most of the crater data on other outer planet satellites has a lower diameter limit of about 10 km and represents the period of late heavy bombardment which is not preserved on Triton. Consequently, trying to deduce the origin of crater populations on other satellites (except Miranda) by comparing them with the Triton population is probably not possible until better data are obtained from the Galileo and Cassini missions.

## REFERENCES AND NOTES


1. B. A. Smith *et al.*, *Science* **246**, 1422 (1989).
2. Transition diameters on the icy satellites have been discussed by several authors, including C. R. Chapman and W. B. McKinnon in *Satellites*, J. A. Burns and M. S. Shapley, Eds. (Univ. of Arizona Press, Tucson, AZ, 1986), pp. 492–580; S. K. Croft, *Lunar Planet. Sci.* **19**, 219 (1988); and P. M. Schenk, *J. Geophys. Res.* **94**, 3813 (1989). The transition diameter and uncertainty given in the text for Triton are based on the morphologies of 12 craters between 6 and 20 km in diameter, including those in Fig. 1. The depth-diameter curves in Fig. 1 are derived from shadow-depth measurements from Croft (1988) and unpublished data. The Rhea curve differs slightly from the Rhea curve of Schenk (1989).
3. The *R* plot displays information on the differential size distribution. On this type of plot a horizontal line has a differential −3 slope; one sloping down to the left at 45° has a differential −2 slope and one sloping down to the right at 45° has a differential −4 slope. The vertical position of the curve on an *R* plot is a measure of crater density; the higher the curve, the greater the crater density. Error bars are defined as $R/N^{0.5}$, where $N$ is the number of craters used to compute $R$. For more details see Crater Analysis Techniques Working Group, *Icarus* **37**, 467 (1978).
4. S. K. Croft, *Lunar Planet. Sci.* **21**, 246 (1990); J. S. Kargel and R. G. Strom, *ibid.*, p. 599.
5. S. K. Croft, *ibid.* **19**, 223 (1988).
6. R. Greenberg *et al.*, in *Uranus* (Univ. of Arizona Press, Tucson, AZ, in press).
7. W. B. McKinnon, *Nature* **311**, 355 (1984); P. Goldreich *et al.*, *Science* **245**, 500 (1989).


9 August 1990; accepted 24 September 1990